Biometrika (2016), **xx**, x, *pp*. 1–15

Printed in Great Britain

Exact simulation of max-stable processes

BY CLÉMENT DOMBRY
Université de Franche–Comté, Laboratoire de Mathématiques de Besançon, UMR CNRS 6623, 16 Route de Gray, 25030 Besançon cedex, France
clement.dombry@univ-fcomte.fr

SEBASTIAN ENGELKE
École Polytechnique Fédérale de Lausanne, EPFL-FSB-MATHAA-STAT, Station 8, 1015 Lausanne, Switzerland
sebastian.engelke@epfl.ch

AND MARCO OESTING
Universität Siegen, Department Mathematik, Walter-Flex-Str. 3, 57068 Siegen, Germany
oesting@mathematik.uni-siegen.de

SUMMARY

Max-stable processes play an important role as models for spatial extreme events. Their complex structure as the pointwise maximum over an infinite number of random functions makes their simulation difficult. Algorithms based on finite approximations are often inexact and computationally inefficient. We present a new algorithm for exact simulation of a max-stable process at a finite number of locations. It relies on the idea of simulating only the extremal functions, that is, those functions in the construction of a max-stable process that effectively contribute to the pointwise maximum. We further generalize the algorithm by Dieker & Mikosch (2015) for Brown–Resnick processes and use it for exact simulation via the spectral measure. We study the complexity of both algorithms, prove that our new approach via extremal functions is always more efficient, and provide closed-form expressions for their implementation that cover most popular models for max-stable processes and multivariate extreme value distributions. For simulation on dense grids, an adaptive design of the extremal function algorithm is proposed.

Some key words: Exact simulation; Extremal function; Extreme value distribution; Max-stable process; Spectral measure.

1. INTRODUCTION

Max-stable processes have become widely used for modelling spatial extreme events. Occurring naturally in the context of extremes as limits of maxima of independent copies of stochastic processes, they have found many applications in environmental science; see for instance Coles (1993), Buishand et al. (2008), Blanchet & Davison (2011) and Davison et al. (2012).

Any sample continuous max-stable process Z with unit Fréchet margins on some compact domain $\mathcal{X} \subset \mathbb{R}^d$ is characterized by a point process representation (de Haan, 1984)

$$Z(x) = \max_{i \geq 1} \zeta_i \psi_i(x), \quad x \in \mathcal{X}, \tag{1}$$

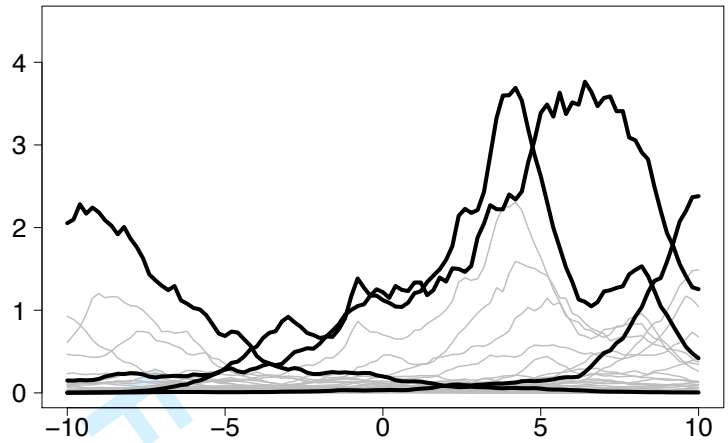

Fig. 1. The Poisson process $\{(\zeta_i, \psi_i), i \geq 1\}$ (grey). Only finitely many (bold black) (ζ_i, ψ_i) contribute to the maximum process Z.

where $\{(\zeta_i, \psi_i), i = 1, 2, \dots\}$ is a Poisson process on $(0, \infty) \times \mathcal{C}$ with intensity measure $\zeta^{-2}\mathrm{d}\zeta \times \nu(\mathrm{d}\psi)$ for some locally finite measure ν on the space $\mathcal{C} = \mathcal{C}\{\mathcal{X}, [0, \infty)\}$ of continuous nonnegative functions on $\mathcal{X}$ such that

$$\int_{\mathcal{C}} \psi(x)\nu(\mathrm{d}\psi) = 1, \quad x \in \mathcal{X}. \tag{2}$$

Figure 1 shows a realization of Z composed of those random functions of the above point process that are maximal at some location. Due to this complex structure of max-stable processes, in many cases, analytical expressions are only available for lower-dimensional distributions and related characteristics need to be assessed by simulation. Moreover, non-conditional simulation is an important part of conditional simulation procedures that can be used to predict extreme events given some additional information (e.g., Dombry et al., 2013; Oesting & Schlather, 2014). Thus, there is a need for fast and accurate simulation algorithms.

As the spectral representation (1) involves an infinite number of functions, exact simulation of Z is in general not straightforward and finite approximations are used in practice. For the widely-used Brown–Resnick processes (Kabluchko et al., 2009), Engelke et al. (2011) and Oesting et al. (2012) exploit the fact that the representation (1) is not unique in order to propose simulation procedures based on equivalent representations. However, often these approximations do not provide satisfactory results in terms of accuracy or computational effort. The effect of the approximation can be illustrated in Fig. 1, where an approximate algorithm might miss one or several of the bold black processes and the resulting maximum process would be strictly smaller than the exact realization Z.

Exact simulation procedures can so far be implemented only in special cases. Schlather (2002) proposes an algorithm that simulates the points $\{\zeta_i, i \geq 1\}$ in (1) in descending order until some stopping rule takes effect. If ν is the probability measure of a stochastic process whose supremum on $\mathcal{X}$ is almost surely bounded or if Z is a mixed moving maxima process with uniformly bounded and compactly supported shape function, this procedure allows exact simulation of Z. For extremal-t processes (Opitz, 2013), the elliptical structure of Gaussian processes can be ex-

ploited to obtain exact samples (Thibaud & Opitz, 2015). M. Oesting, M. Schlather and C. Zhou (arXiv:1310.1813v1) focus on a class of equivalent representations for general max-stable processes that, in principle, allow for optimally efficient exact simulation. They propose to simulate max-stable processes via the normalized spectral representation with all the spectral functions sharing the same supremum. Being efficient with respect to the number of spectral functions, the simulation of a single normalized function might be rather intricate in some cases, including Brown–Resnick processes. For the latter, Dieker & Mikosch (2015) derived a representation that enables exact simulation at finitely many locations.

Several articles focus on the simulation of finite dimensional max-stable distributions or, equivalently, of their associated extreme value copula. Ghoudi et al. (1998) and Capéraà et al. (2000) propose simulation procedures for certain bivariate extreme value distributions. Stephenson (2003) considers extreme value distributions of logistic type. Boldi (2009) provides a method for exact simulation from the spectral measure of extremal Dirichlet and logistic distributions.

In this paper, we consider exact simulation of a general max-stable process Z at a finite number of locations. We introduce a new procedure based on the idea of simulating only the extremal functions (cf. Dombry & Éyi-Minko, 2012, 2013) out of the infinite set $\{\zeta_i\psi_i, i \geq 1\}$, i.e., those functions that satisfy $\zeta_i\psi_i(x) = Z(x)$ for some $x \in \mathcal{X}$; i.e., the bold black functions in Fig. 1. In contrast to all existing simulation procedures, the process Z is not simulated simultaneously, but successively at different locations, rejecting all those functions that are not compatible with the process at the locations simulated so far. We propose also a second procedure that relies on sampling from the spectral measure on the L_1-sphere of a multivariate extreme value distribution. Interestingly, in the case of Brown–Resnick processes, this second procedure is identical to the algorithm by Dieker & Mikosch (2015). We prove that the new procedure based on extremal functions is computationally more efficient than simulation via the spectral measure. Both procedures are based on random functions following the same type of distribution that can be easily simulated for most popular max-stable models. Both algorithms also apply very efficiently to exact simulation of finite-dimensional max-stable distributions or, equivalently, of the associated extreme value copulas.

2. Simulation via extremal functions

In §§2 and 3, we propose two procedures for exact simulation of arbitrary max-stable processes and distributions. More precisely, for a fixed number $N \in \mathbb{N}$ of distinct locations $x = (x_1, \ldots, x_N) \in \mathcal{X}^N$, we aim at exact simulation of the max-stable random vector

$$Z(x) = \{Z(x_1), \ldots, Z(x_N)\}, \tag{3}$$

where Z is a sample-continuous process given by the spectral representation (1). Without loss of generality, we may consider only processes with unit Fréchet margins, as any sample-continuous max-stable process can be obtained from a process with unit Fréchet margins via marginal transformations. The first procedure, presented in this section, relies on conditional distributions of the Poisson process underlying the max-stable process. This allows exact simulation of (3) by simulating at each location only the unique function that actually attains the maximum, see Fig. 1. Below, we briefly present some results on the distribution of this function, the so-called extremal function. Throughout, we write $f(x) = \{f(x_1), \ldots, f(x_N)\}$ for the restriction of a generic, possibly random, function f to the locations $x \in \mathcal{X}^N$.

Starting from representation (1), we use a point process approach and recall that the $\mathcal{C}$-valued point process $\Phi = \{\phi_i\}_{i\geq 1}$ with $\phi_i = \zeta_i \psi_i$ is a Poisson point process with intensity

$$\mu(A) = \int_{\mathcal{C}} \int_0^\infty 1_{\{\zeta\psi \in A\}} \zeta^{-2} \, \mathrm{d}\zeta \, \nu(\mathrm{d}\psi), \quad A \subset \mathcal{C} \text{ Borel}, \tag{4}$$

where $1_{\{L\}}$ denotes the indicator function of a logical expression L, i.e. $1_{\{L\}} = 1$ if L is true and $1_{\{L\}} = 0$ otherwise.

DEFINITION 1. *Let $K \subset \mathcal{X}$ be nonempty and compact. A function $\phi \in \Phi$ is called K-extremal if there is some $x \in K$ such that $\phi(x) = Z(x)$; otherwise it is called K-subextremal. We denote by Φ_K^+ the set of K-extremal functions and by Φ_K^- the set of K-subextremal functions.*

It can be shown that Φ_K^+ and Φ_K^- are properly defined Poisson point processes. When $K = \{x_0\}$, $x_0 \in \mathcal{X}$, is reduced to a single point, it is easy to show that $\Phi_{\{x_0\}}^+$ is also almost surely reduced to a single point which we denote by $\phi_{x_0}^+$, termed the extremal function at x_0. The distribution of $\phi_{x_0}^+$ is given in the next proposition.

PROPOSITION 1 (DOMBRY & ÉYI-MINKO (2013), PROPOSITION 4.2). *The random variables $Z(x_0)$ and $\phi_{x_0}^+/Z(x_0)$ are independent. Furthermore, $Z(x_0)$ has a unit Fréchet distribution and the distribution of $\phi_{x_0}^+/Z(x_0)$ is*

$$P_{x_0}(A) = \operatorname{pr}\left\{\phi_{x_0}^+/Z(x_0) \in A\right\} = \int_{\mathcal{C}} 1_{\{f/f(x_0)\in A\}} f(x_0) \, \nu(\mathrm{d}f), \quad A \subset \mathcal{C} \text{ Borel}. \tag{5}$$

By definition, $\phi_{x_0}^+(x_0) = Z(x_0)$, so the distribution P_{x_0} is supported by the subset of functions $\{f \in \mathcal{C}, f(x_0) = 1\}$.

PROPOSITION 2. *The restricted point process $\Phi \cap \{f \in \mathcal{C}, f(x_0) > 0\}$ is a Poisson process with intensity*

$$\int_A 1_{\{f(x_0)>0\}} \mu(\mathrm{d}f) = \int_{\mathcal{C}} \int_0^\infty 1_{\{\zeta f \in A\}} \zeta^{-2} \, \mathrm{d}\zeta \, P_{x_0}(\mathrm{d}f), \quad A \subset \mathcal{C} \text{ Borel}. \tag{6}$$

Remark 1. As a consequence of (6), independent copies $Y_1, Y_2, \ldots$ of processes with distribution P_{x_0} result in a point process $\{\zeta_i Y_i\}_{i\geq 1}$ which has the same distribution as the restricted point process $\Phi \cap \{f \in \mathcal{C}, f(x_0) > 0\}$. If $\nu(\{f \in \mathcal{C}, f(x_0) = 0\}) = 0$, then Φ consists only of functions with positive value at x_0 and Φ has the same distribution as $\{\zeta_i Y_i\}_{i\geq 1}$. This provides an alternative point process representation of the max-stable process Z in terms of a random process Y such that $Y(x_0) = 1$ almost surely. Engelke et al. (2014, 2015) exploit this representation for statistical inference on Z.

These preliminary considerations enable us to introduce a procedure for exact simulation of the max-stable process Z at locations $x \in \mathcal{X}^N$. For $n = 1, \ldots, N$ we consider the extremal and subextremal point processes $\Phi_n^+ = \Phi_{\{x_1,\ldots,x_n\}}^+$ and $\Phi_n^- = \Phi_{\{x_1,\ldots,x_n\}}^-$. We have that Φ_n^+ equals $\{\phi_{x_i}^+\}_{1\leq i\leq n}$, where the cardinality of this set may be less than n as several locations may share the same extremal function. We define the nth-step maximum process

$$Z_n(x) = \max_{\phi\in\Phi_n^+} \phi(x) = \max_{1\leq i\leq n} \phi_{x_i}^+(x), \quad x \in \mathcal{X}. \tag{7}$$

By the definition of extremal functions we have $Z(x_i) = \phi_{x_i}^+(x_i)$ and clearly

$$Z(x_i) = Z_n(x_i) \quad (i = 1, \ldots, n). \tag{8}$$

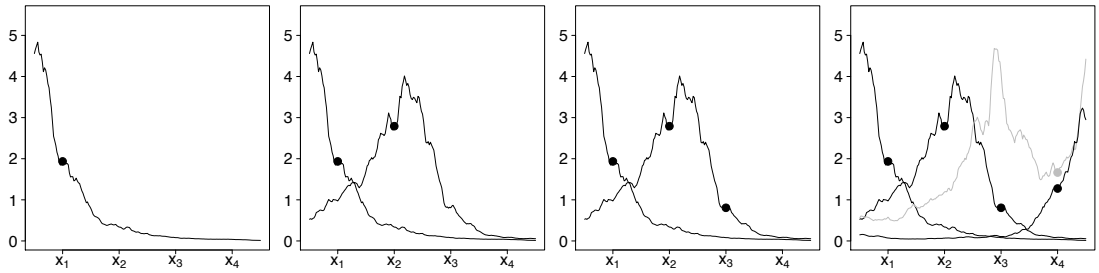

Fig. 2. Simulation of Z via Algorithm 1 at locations (x_1, x_2, x_3, x_4). The initial process $\phi^+_{x_1}$ is always accepted (first panel). The second process $\phi^+_{x_2}$ is accepted as it exceeds $Z_1 = \phi^+_{x_1}$ at x_2 but not at x_1 (second panel). The third process $\phi^+_{x_3}$ is equal to $\phi^+_{x_2}$ since $\tilde{\Phi}_3 = \emptyset$ (third panel). The first sample of P_{x_4} (grey line) is rejected since it exceeds Z_3 at x_3; the second sample is valid and thus called $\phi^+_{x_4}$ (fourth panel).

Hence, in order to exactly simulate Z at locations x, it is enough to simulate Φ^+_N exactly. We will proceed inductively and simulate the sequence $(\phi^+_{x_n})_{1\le n\le N}$ according to the following theorem.

THEOREM 1. *The distribution of $(\phi^+_{x_n})_{1\le n\le N}$ is given by the following sequential procedure. The initial distribution for the extremal function $\phi^+_{x_1}$ has the same distribution as $F_1 Y_1$ where F_1 is a unit Fréchet random variable and Y_1 an independent random process with distribution P_{x_1} given by* (5).

For $n = 1, \dots, N-1$, the conditional distribution of $\phi^+_{x_{n+1}}$ given $(\phi^+_{x_i})_{1\le i\le n}$ is equal to the distribution of

$$\tilde{\phi}^+_{x_{n+1}} = \begin{cases} \operatorname{argmax}_{\phi\in\tilde{\Phi}_{n+1}} \phi(x_{n+1}), & \tilde{\Phi}_{n+1} \neq \emptyset, \\ \operatorname{argmax}_{\phi\in\Phi^+_n} \phi(x_{n+1}), & \tilde{\Phi}_{n+1} = \emptyset, \end{cases}$$

where $\tilde{\Phi}_{n+1}$ is a Poisson process with intensity

$$1_{\{f(x_i)<Z_n(x_i),\ i=1,\dots,n\}} 1_{\{f(x_{n+1})>Z_n(x_{n+1})\}} \mu(\mathrm{d}f) \tag{9}$$

and Z_n is defined by (7).

From the Theorem 1 one can deduce Algorithm 1 for exact simulation of the max-stable process Z at locations $x = (x_1, \dots, x_N)$. According to Proposition 2 and Remark 1, the distribution $P_{x_{n+1}}$ can be used to simulate $\tilde{\Phi}_{n+1}$ with intensity (9). Hence, the algorithm requires only that one can simulate from the distributions $P_{x_1}, \dots P_{x_N}$, which can be easily done for the most popular max-stable models. See §4 for details. Figure 2 illustrates the procedure.

3. SIMULATION VIA THE SPECTRAL MEASURE

Dieker & Mikosch (2015) presented a procedure for exact simulation of the finite-dimensional distributions of stationary Brown–Resnick processes. Applying change of measure arguments for Gaussian processes, they found an alternative representation of these processes that can be simulated easily. In this section, we introduce an approach relying on the spectral representation on the L_1-sphere that can be applied for general max-stable distributions. In the case of stationary Brown–Resnick processes, in Remark 3 we retrieve the algorithm of Dieker & Mikosch (2015).

Algorithm 1. Exact simulation of a max-stable process Z at $x = (x_1, \dots, x_N)$ via extremal functions

Simulate $\zeta^{-1} \sim \mathrm{Exp}(1)$ and $Y \sim P_{x_1}$.
Set $Z(x) = \zeta Y(x)$.
For $n = 2, \dots, N$:
  Simulate $\zeta^{-1} \sim \mathrm{Exp}(1)$.
  While $\zeta > Z(x_n)$ {
    Simulate $Y \sim P_{x_n}$.
    If $\zeta Y(x_i) < Z(x_i)$ for all $i = 1, \dots, n-1$,
      update $Z(x)$ to the componentwise maximum $\max\{Z(x), \zeta Y(x)\}$.
    Simulate $e \sim \mathrm{Exp}(1)$ and update ζ^{-1} to $\zeta^{-1} + e$.
  }
Return Z.

Let us recall the spectral decomposition of the max-stable random vector $Z(x)$ with $x \in \mathcal{X}^N$ (Resnick, 2008, Chap. 5). Following Equation (1), $Z(x) = \max_{i \geq 1} \zeta_i \psi_i(x)$ is generated by the Poisson process $\Phi_x = \{\zeta_i \psi_i(x), i = 1, 2, \dots\}$ whose intensity measure on the cone $D = [0, \infty)^N \setminus \{0\}$ is denoted by μ_x. Due to its homogeneity, μ_x can be factorized into a radial part on $(0, \infty)$ and an angular part on the unit L_1-sphere $S_{N-1} = \{z \in D, \|z\| = 1\}$, where $\|z\| = z_1 + \cdots + z_N$, for $z = (z_1, \dots, z_N) \in D$. More precisely, a change to polar coordinates under the map $U : D \to (0, \infty) \times S_{N-1}$, $U(z) = (\|z\|, z/\|z\|)$ yields

$$\mu_x(F) = \int_{U(F)} \mu_x \circ U^{-1}(\mathrm{d}r, \mathrm{d}s) = N \int_{U(F)} r^{-2} \mathrm{d}r H(\mathrm{d}s), \tag{10}$$

for any Borel subset $F \subset D$. The probability measure H on S_{N-1} is called the spectral measure of $Z(x)$, and it satisfies

$$\int_{S_{N-1}} s_j H(ds) = N^{-1} \quad (j = 1, \dots, N).$$

Equation (10) shows that we can represent the process Φ_x as

$$\Phi_x = \{U^{-1}(R_i, Q_i), i = 1, 2, \dots\} = \{R_i Q_i, i = 1, 2, \dots\}, \tag{11}$$

where $\{R_i, i = 1, 2, \dots\}$ is a Poisson process on $(0, \infty)$ with intensity $N r^{-2} \mathrm{d}r$ and $Q_1, Q_2, \dots$ are independently sampled from the spectral measure H on S_{N-1}. The advantage of this representation is that the components of Q_i are bounded by 1. This ensures that $Z(x) = \max_{i \geq 1} R_i Q_i$ can be simulated exactly by generating the largest R_i first until none of the remaining points $R_i Q_i$ can contribute to the maximum.

The only difficulty is thus to generate the random variables Q_i from the probability measure H on the $(N-1)$-dimensional positive sphere S_{N-1}. The following theorem gives such an explicit representation for the Q_i for general max-stable distributions $Z(x)$ based on the distributions P_{x_k} $(k = 1, \dots, N)$ in (5).

THEOREM 2. *Let $T_1, T_2, \dots$ be independent copies of a random variable T with uniform distribution on the discrete set $\{1, \dots, N\}$. Further, for any $k = 1, \dots, N$, let $Y_1^{(k)}, Y_2^{(k)}, \dots$ be independent random processes with distribution P_{x_k} as in* (5)*. Then, the S_{N-1}-valued random*

variables

$$Q_i = \frac{Y_i^{(T_i)}(x)}{\|Y_i^{(T_i)}(x)\|} \quad (i = 1, 2, \ldots),$$

are independent with distribution H. *Consequently, with* $\{R_i,\ i = 1, 2, \ldots\}$ *as above,*

$$Z(x) = \max_{i \geq 1} R_i \frac{Y_i^{(T_i)}(x)}{\|Y_i^{(T_i)}(x)\|}. \tag{12}$$

Theorem 2 shows how to simulate from the spectral measure H. It requires only to be able to simulate from the distributions P_{x_k} $(k = 1, \ldots, N)$. Algorithm 2, an adaptation of Schlather's (2002) algorithm, provides an exact sample from the max-stable process Z at locations x.

Algorithm 2. Exact simulation of a max-stable process Z at $x = (x_1, \ldots, x_N)$

Simulate $\zeta^{-1} \sim \mathrm{Exp}(N)$ and set $Z(x) = 0$.
While $\zeta > \min\{Z(x_1), \ldots, Z(x_N)\}$
  Simulate T uniform on $\{1, \ldots, N\}$ and Y according to the law P_{x_T}.
  Update $Z(x)$ by the componentwise maximum $\max\{Z(x), \zeta Y(x)/\|Y(x)\|\}$.
  Simulate $e \sim \mathrm{Exp}(N)$ and update ζ^{-1} by $\zeta^{-1} + e$.
Return Z.

Both Algorithm 1 and Algorithm 2 include the simulation of random functions with distributions P_{x_0} in (5), for $x_0 \in \mathcal{X}$. In §4 we provide closed-form expressions for various important examples of max-stable process and multivariate extreme value distributions.

4. Examples

4·1. *Moving maximum process*

All proofs of this section can be found in the Supplementary Material. The parameter space is $\mathcal{X} = \mathbb{Z}^d$ or $\mathbb{R}^d$ and λ denotes the counting measure or the Lebesgue measure, respectively. A moving maximum process on $\mathcal{X}$ is a max-stable process of the form

$$Z(x) = \max_{i \geq 1} \zeta_i h(x - \chi_i), \quad x \in \mathcal{X}, \tag{13}$$

where $\{(\zeta_i, \chi_i), i = 1, 2, \ldots\}$ is a Poisson process on $(0, \infty) \times \mathcal{X}$ with intensity measure $\zeta^{-2} \mathrm{d}\zeta \times \lambda(\mathrm{d}\chi)$ and $h : \mathcal{X} \to [0, \infty)$ is a continuous function satisfying $\int_{\mathcal{X}} h(x)\lambda(\mathrm{d}x) = 1$. A popular example is the Gaussian extreme value process proposed in a 1990 University of Surrey technical report by R. L. Smith, where h is a multivariate Gaussian density on $\mathbb{R}^d$.

Proposition 3. *Consider the moving maximum process* (13). *For all* $x_0 \in \mathcal{X}$, *the distribution* P_{x_0} *is equal to the distribution of the random function*

$$\frac{h(\cdot + \chi - x_0)}{h(\chi)}, \quad \chi \sim h(u)\lambda(\mathrm{d}u).$$

4·2. *Brown–Resnick process*

We consider max-stable processes obtained by representation (1) where ν is a probability measure on $\mathcal{C}$ given by

$$\nu(A) = \mathrm{pr}\left[\exp\left\{W(\cdot) - \sigma^2(\cdot)/2\right\} \in A\right], \quad A \subset \mathcal{C} \text{ Borel}, \tag{14}$$

with W a sample-continuous centred Gaussian process on $\mathcal{X}$ with variance $\sigma^2(x) = E\{W(x)^2\}$. In other words, ν is the distribution of the log-normal process $Y(x) = \exp\left\{W(x) - \sigma^2(x)/2\right\}$, $x \in \mathcal{X}$.

An interesting phenomenon arises when $\mathcal{X} = \mathbb{Z}^d$ or $\mathbb{R}^d$ and W has stationary increments: Kabluchko et al. (2009) show that the associated max-stable process Z is then stationary with distribution depending only on the semi-variogram

$$\gamma(h) = \frac{1}{2} E\left[\{W(h) - W(0)\}^2\right], \quad h \in \mathcal{X}.$$

The stationary max-stable process Z is called a Brown–Resnick process. However, our results apply both in the stationary and non-stationary case (cf., Kabluchko, 2011) and unless stated otherwise we do not assume that W has stationary increments.

PROPOSITION 4. *Consider the Brown–Resnick type model* (14). *For all $x_0 \in \mathcal{X}$, the distribution P_{x_0} is equal to the distribution of the log-normal process*

$$\widetilde{Y}(x) = \exp\left[W(x) - W(x_0) - \frac{1}{2}\mathrm{var}\{W(x) - W(x_0)\}\right], \quad x \in \mathcal{X}.$$

Remark 2. The finite-dimensional margins of Brown–Resnick processes are Hüsler & Reiss (1989) distributions and Proposition 4 therefore provides a method for their exact simulation.

Remark 3. For stationary Brown–Resnick processes, i.e., when W has stationary increments with $W(0) = 0$, it is easy to deduce from Proposition 4 that P_{x_0} is equal to the distribution of

$$\exp\left\{W(x - x_0) - \gamma(x - x_0)\right\}, \quad x \in \mathcal{X}.$$

Thus, Theorem 2 yields

$$Z(x) = \max_{i \geq 1} R_i \frac{\exp\{W_i(x - T_i) - \gamma(x - T_i)\}}{\sum_{\ell=1}^{N} \exp\{W_i(x_\ell - T_i) - \gamma(x_\ell - T_i)\}}$$

where $\{R_i : i = 1, 2, \dots\}$ is a Poisson process on $(0, \infty)$ with intensity $Nr^{-2}\mathrm{d}r$, $T_1, T_2, \dots$ are independent with uniform distribution on $\{x_1, \dots, x_N\}$ and $W_1, W_2, \dots$ are independent copies of W. The same representation appears in Dieker & Mikosch (2015), so Algorithm 2 is identical to the Dieker and Mikosch procedure in this case.

4·3. *Extremal-t process*

We consider the so-called extremal-t max-stable process (cf., Opitz, 2013) defined by representation (1) with ν the distribution of the random process

$$Y(x) = c_\alpha \max\{0, W(x)\}^\alpha, \quad x \in \mathcal{X}, \tag{15}$$

where $\alpha > 0$, $c_\alpha = \pi^{1/2} 2^{-(\alpha-2)/2} / \Gamma\left\{(1 + \alpha)/2\right\}$, and W a sample-continuous centred Gaussian process on $\mathcal{X}$ with unit variance and covariance function K. For $\alpha = 1$, the corresponding max-stable process in (1) coincides with the widely-used extremal Gaussian process by Schlather (2002).

PROPOSITION 5. *Consider the extremal-t model* (15). *For all $x_0 \in \mathcal{X}$, the distribution P_{x_0} is equal to the distribution of* $\max(T, 0)^\alpha$, *where $T = (T(x))_{x \in \mathcal{X}}$ is a Student process with $\alpha + 1$ degrees of freedom, location and scale functions given respectively by*

$$\mu(x) = K(x_0, x), \quad \hat{K}(x_1, x_2) = \frac{K(x_1, x_2) - K(x_0, x_1)K(x_0, x_2)}{(\alpha + 1)}.$$

4·4. *Multivariate extreme value distributions*

In this section, we review some popular multivariate extreme value distributions, i.e., the case when $\mathcal{X} = \{1, \ldots, N\}$ in (1) is a finite set for some fixed $N \in \mathbb{N}$. For these models, we explicitly calculate the measure P_{j_0} for any $j_0 = 1, \ldots, N$. Unless otherwise stated, all random vectors are N-dimensional in this section. For more details on the models, see Gudendorf & Segers (2010).

The symmetric logistic model in dimension N with parameter $\theta \in (0, 1)$ corresponds to the max-stable random vector with cumulative distribution function

$$\mathrm{pr}(Z \leq z) = \exp\left\{ -\left(\sum\nolimits_{j=1}^{N} z_j^{-1/\theta} \right)^{\theta} \right\}, \quad z = (z_1, \ldots, z_N) \in (0, \infty)^N. \tag{16}$$

PROPOSITION 6. *Let $\beta = 1/\theta$. In the logistic model* (16)*, the probability measure P_{j_0} for any $j_0 = 1, \ldots, N$ is equal to the distribution of the random vector*

$$\left(\frac{F_1}{F_{j_0}}, \ldots, \frac{F_N}{F_{j_0}} \right)$$

where $F_1, \ldots, F_N$ are independent, F_j $(j \neq j_0)$ follows a $\mathrm{Frechet}(\beta, c_\beta)$ *distribution with scale parameter $c_\beta = \Gamma(1 - 1/\beta)^{-1}$ and $(F_{j_0}/c_\beta)^{-\beta}$ follows a* $\mathrm{Gamma}(1 - 1/\beta, 1)$ *distribution.*

Remark 4. The asymmetric logistic distribution can be represented as a mixture of symmetric logistic distributions; see Theorem 1 in Stephenson (2003), for instance. As a consequence, Proposition 6 also enables exact simulation of asymmetric logistic distributions.

The negative logistic model in dimension N with parameter $\theta > 0$ corresponds to the max-stable random vector Z with cumulative distribution function

$$\mathrm{pr}(Z \leq z) = \exp\left\{ \sum_{\emptyset \neq J \subset \{1, \ldots, N\}} (-1)^{|J|} \left(\sum\nolimits_{j \in J} z_j^{\theta} \right)^{-1/\theta} \right\}, \quad z \in (0, \infty)^N. \tag{17}$$

PROPOSITION 7. *In the negative logistic model* (17)*, the probability measure P_{j_0} for any $j_0 = 1, \ldots, N$ is equal to the distribution of the random vector*

$$\left(\frac{W_1}{W_{j_0}}, \ldots, \frac{W_N}{W_{j_0}} \right)$$

where $W_1, \ldots, W_N$ are independent, W_j $(j \neq j_0)$ follows a $\mathrm{Weibull}(\theta, c_\theta)$ *distribution with scale parameter $c_\theta = \Gamma(1 + 1/\theta)^{-1}$ and $(W_{j_0}/c_\theta)^{\theta}$ follows a $\Gamma(1 + 1/\theta, 1)$ distribution.*

The Dirichlet mixture model was introduced by Boldi & Davison (2007). In dimension N, the model corresponds to the max-stable random vector given by

$$Z = \max_{i \geq 1} \zeta_i (N Y_i) \tag{18}$$

where the Y_is are independent identically distributed random vectors on the simplex

$$S_{N-1} = \left\{ y \in [0, 1]^n, \sum\nolimits_{j=1}^{N} y_j = 1 \right\}.$$

The distribution of each Y_i is a mixture of m Dirichlet models, i.e., its Lebesgue density is of the form

$$h(y) = \sum_{k=1}^{m} \pi_k \mathrm{diri}(y \mid \alpha_{1k}, \ldots, \alpha_{Nk}), \quad y = (y_1, \ldots, y_N) \in S_{N-1}, \tag{19}$$

where $\pi_k \geq 0, k = 1, \ldots, m$ such that $\sum_{k=1}^m \pi_k = 1, \alpha_{ik} > 0\,(i = 1, \ldots, N; k = 1, \ldots, m)$ and

$$\mathrm{diri}(y \mid \alpha_1, \ldots, \alpha_N) = \frac{1}{B(\alpha)} \prod_{j=1}^N y_j^{\alpha_j - 1}, \quad B(\alpha) = \frac{\prod_{j=1}^N \Gamma(\alpha_j)}{\Gamma(\sum_{j=1}^N \alpha_j)}. \tag{20}$$

Here, the parameters π_k and α_{ik} $(i = 1, \ldots, N; k = 1, \ldots, m)$ are such that

$$E(Y_j) = \sum_{k=1}^m \pi_k \frac{\alpha_{jk}}{\sum_{i=1}^N \alpha_{ik}} = \frac{1}{N} \quad (j = 1, \ldots, N).$$

PROPOSITION 8. *In the Dirichlet model* (18)*, we have for any* $j_0 = 1, \ldots, N$ *that* $P_{j_0} = \sum_{k=1}^m N \hat{\pi}_k P_{j_0}^{(k)}$ *where* $\hat{\pi}_k = \pi_k \alpha_{j_0 k} / (\sum_{i=1}^N \alpha_{ik})$ *and* $P_{j_0}^{(k)}$ *is equal to the distribution of the random vector*

$$\left(\frac{G_1^{(k)}}{G_{j_0}^{(k)}}, \ldots, \frac{G_N^{(k)}}{G_{j_0}^{(k)}} \right)$$

and $G_1^{(k)}, \ldots, G_N^{(k)}$ *are independent random variables with*

$$G_{j_0}^{(k)} \sim \mathrm{Ga}(\alpha_{j_0 k} + 1, 1), \quad G_j \sim \mathrm{Ga}(\alpha_{jk}, 1), \quad j \neq j_0.$$

5. COMPLEXITY OF THE ALGORITHMS

In this section, we assess the complexity of Algorithms 1 and 2 as a function of the number N of simulation sites. Both algorithms contain the simulation of exponential random variables e and the simulation of N-dimensional random vectors $Y(x)$ according to a mixture of the laws $P_{x_1}, \ldots, P_{x_N}$. The simulation of e causes much less computational effort than the simulation of Y and can therefore be neglected in the analysis of the algorithmic complexity. We thus consider the number $C_1(N)$ and $C_2(N)$ of random vectors $Y(x)$ that must be simulated by Algorithm 1 and 2 respectively to obtain one exact simulation of $Z(x)$. The following proposition provides simple expressions for the expectations $E\{C_1(N)\}$ and $E\{C_2(N)\}$.

PROPOSITION 9. *The expected number of random vectors* $Y(x)$ *that are needed for exact simulation of* Z *at* $x = (x_1, \ldots, x_N)$ *are:*

Algorithm 1: $E\{C_1(N)\} = N$;

Algorithm 2: $E\{C_2(N)\} = NE\left\{ \max_{i=1,\ldots,N} Z(x_i)^{-1} \right\}$.

Furthermore, $E\{C_1(N)\} \leq E\{C_2(N)\}$*, with equality if and only if* $Z(x_1) = \cdots = Z(x_N)$ *almost surely.*

The expectation of $C_2(N)$ can be calculated similarly to Proposition 4.8 in the 2013 technical report by M. Oesting, M. Schlather and C. Zhou (arXiv:1310.1813v1). The proof for the expectation of $C_1(N)$ is more difficult and is provided in the Supplementary Material.

Remark 5. Tthe expectation of $C_1(N)$ does not depend on $Z(x)$. Further characteristics of its distribution such as its variance, however, depend strongly on the model and apparently cannot be readily expressed by an explicit formula in the general case. The following simple examples may provide some further insight into the distribution of $C_1(N)$. In the case of independent random variables $Z(x_i)$ $(i = 1, \ldots, N)$, the extremal function at x_i is $x \mapsto Z(x_i) 1_{\{x = x_i\}}$ which

ε	$\bar{\mu}_1$	$\bar{\mu}_2$	$\bar{\sigma}_1$	$\bar{\sigma}_2$
0.25	291	1037	195	605
0.5	79	260	53	149
1	25	68	15	40
2	9	21	5	12

Table 1. *Empirical means $\bar{\mu}_1$ and $\bar{\mu}_2$ and standard deviations $\bar{\sigma}_1$ and $\bar{\sigma}_2$ of the number of random vectors to be simulated to obtain an exact sample of a Brown–Resnick process on the grid $(\varepsilon\mathbb{Z} \cap [-2, 2]) \times (\varepsilon\mathbb{Z} \cap [-2, 2])$ via Algorithm 1 and Algorithm 2, respectively.*

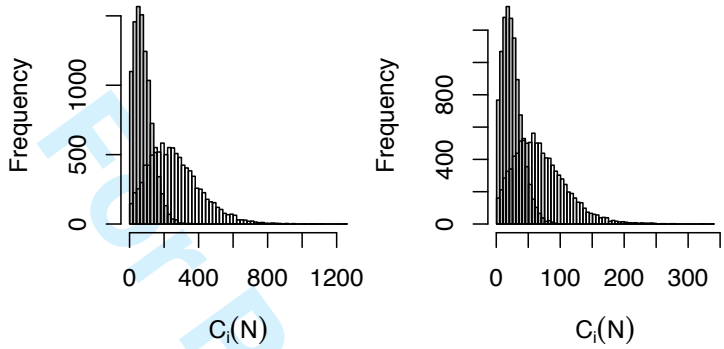

Fig. 3. Histograms for $C_1(N)$ (grey) and $C_2(N)$ (white) based on 10000 exact simulations of a Brown–Resnick process on the grid $(\varepsilon\mathbb{Z} \cap [-2, 2]) \times (\varepsilon\mathbb{Z} \cap [-2, 2])$ for $\varepsilon = 1$ (left) and $\varepsilon = 0.5$ (right), respectively.

is why, at each step of Algorithm 1, a new extremal function is simulated and accepted, whence $C_1(N) \equiv N$. In contrast, for completely dependent random variables $Z(x_i) \equiv Z(x_1)$, there is only one extremal function, namely the constant function $x \mapsto Z(x_1)$, the one simulated at the first location. At each further step of Algorithm 1, all proposed extremal functions are rejected. The number $C_1(N)$ follows a geometric distribution with success probability $1/N$ and, thus, $E\{C_1(N)\} = N$ and $\mathrm{var}\{C_1(N)\} = N(N-1)$. In this case, $C_1(N)$ and $C_2(N)$ share not only the same mean, cf. Proposition 9, but also the same distribution.

We conclude this section with some comments on the complexity of our algorithms and a comparison with other exact simulation procedures. Proposition 9 shows that, for any max-stable process, Algorithm 1 is more efficient than Algorithm 2 in terms of the expected number of simulated functions. As the spectral functions follow either the laws $P_{x_1}, \ldots, P_{x_N}$ or a mixture of these, the simulation of a single spectral function is equally complex in both cases. Thus, the new Algorithm 1 based on extremal functions is always preferable to Algorithm 2.

The differences in complexity of the two algorithms are further illustrated in a simulation study. We consider exact simulations of the Brown–Resnick process associated to the variogram $\gamma(h) = \|h\|$ on a grid $(\varepsilon\mathbb{Z} \cap [-2, 2]) \times (\varepsilon\mathbb{Z} \cap [-2, 2])$. For $\varepsilon \in \{0.25, 0.5, 1, 2\}$, Algorithms 1 and 2 are run 10000 times. The empirical means $\bar{\mu}_1$ and $\bar{\mu}_2$ and standard deviations $\bar{\sigma}_1$ and $\bar{\sigma}_2$ of $C_1(N)$ and $C_2(N)$, respectively, are reported in Table 1. Both the mean and the standard deviation are much larger for Algorithm 2. The corresponding histograms for $C_1(N)$ and $C_2(N)$ are displayed in Fig. 3 for the cases $\varepsilon = 0.5$ and $\varepsilon = 1$.

Finally, we briefly comment on exact simulation via the normalized spectral representation proposed by M. Oesting, M. Schlather and C. Zhou. By Proposition 4.8 in their 2013 technical

report (arXiv:1310.1813v1), the number $C_3(N)$ of simulated normalized spectral functions in this algorithm satisfies

$$E\{C_3(N)\} = \left\{ \int \max_{i=1,\dots,N} \psi(x_i) \nu(\mathrm{d}\psi) \right\} E\left\{ \max_{i=1,\dots,N} Z(x_i)^{-1} \right\} \tag{21}$$

and, thus, depends both on the geometry of the set $\{x_1, \dots, x_N\}$ and on the law of the max-stable process Z. In general, the numbers $E\{C_3(N)\}$ and $E\{C_1(N)\}$ however cannot directly be used to compare the complexity of simulation via the normalized spectral representation and simulation via extremal functions, because the distribution and the simulation complexity of a single random function are different for the two algorithms. As we have seen in §4, the random functions in Algorithms 1 and 2 with distributions P_{x_0} in (5), $x_0 \in \mathcal{X}$, can be simulated efficiently for the most popular max-stable process and extreme value copula models. For the normalized spectral function, exact and efficient algorithms are known only for some cases such as mixed moving maxima processes, but are unavailable in cases like Brown–Resnick or extremal-t processes. For this reason, simulation via Algorithm 1 is often preferable to simulation via the normalized spectral representation even when $E\{C_1(N)\} > E\{C_3(N)\}$.

6. SIMULATION ON DENSE GRIDS

In many applications one is interested in simulating a max-stable process Z on a dense grid, e.g., $x = \mathcal{X} \cap (\varepsilon\mathbb{Z})^d$. As discussed in §5, on average, this requires the simulation of $E\{C_1(N)\} = N$ random functions in Algorithm 1, that is, the simulation of N random vectors of size N. For small ε, N will be large and the procedure can become very time-consuming. Thus, one might be interested in aborting Algorithm 1 after $m < N$ steps, ensuring exactness of the simulation only at locations $x_1, \dots, x_m$. In this case, an alternative design of the algorithm which efficiently chooses the subset of m locations might improve the probability of an exact sample at all N locations.

For comparison of two designs, we introduce the random number

$$N_0 = \min\{m \in \{1, \dots, N\} : Z_m(x) = Z_N(x)\}.$$

For $n \geq N_0$, the algorithm does not provide any new extremal functions, but all the simulated functions are rejected. Hence, N_0 is the optimal number of iterations before aborting the algorithm. One design is preferable to another if its corresponding random number N_0 is stochastically smaller. An efficient design should thus simulate the extremal functions at an early stage of the algorithm. Based on the intuition that $\phi^+_{x_{n+1}}$ is likely not to be contained in Φ^+_n if $Z_n(x_{n+1})$ is small, we propose the following adaptive numbering $x^{(1)}, \dots, x^{(N)}$ of points in Algorithm 1:

$$\begin{aligned} x^{(1)} &= x_1, \\ x^{(n+1)} &= \operatorname{argmin}\left\{ Z_n(x) : x \in \{x_1, \dots, x_N\} \setminus \{x^{(1)}, \dots, x^{(n)}\} \right\} \quad (n = 1, \dots, N-1). \end{aligned} \tag{22}$$

A simulation study indicates that this adaptive version is clearly preferable to Algorithm 1 with a deterministic numbering of locations. The advantage is particularly big in the case of strong dependence, which corresponds to simulation on dense grids. More details on the simulation study and its results are provided in the Supplementary Material.

ACKNOWLEDGEMENT

We thank the editorial team and three referees for helpful comments, and the Swiss National Science Foundation and the Agence Nationale de la Recherche project McSim for financial support.

SUPPLEMENTARY MATERIAL

Supplementary material available at *Biometrika* online includes the proof of Proposition 9, the proofs of all propositions of §4 and the results of the simulation study in §6.

APPENDIX

Proof of Proposition 2. The fact that the restricted point process $\Phi \cap \{f \in \mathcal{C}, f(x_0) > 0\}$ is a Poisson process with intensity $1_{\{f(x_0)>0\}}\mu(\mathrm{d}f)$ is standard. We prove (6). For $A \subset \mathcal{C}$ Borel,

$$\begin{aligned}\int_{\mathcal{C}}\int_0^\infty 1_{\{\zeta f\in A\}}\zeta^{-2}\mathrm{d}\zeta\, P_{x_0}(\mathrm{d}f) &= \int_{\mathcal{C}}\int_0^\infty 1_{\{\zeta f/f(x_0)\in A\}}\zeta^{-2}\mathrm{d}\zeta\, f(x_0)\,\nu(\mathrm{d}f)\\ &= \int_{\mathcal{C}}\int_0^\infty 1_{\{\tilde\zeta f\in A\}}\tilde\zeta^{-2}\mathrm{d}\tilde\zeta\, 1_{\{f(x_0)>0\}}\,\nu(\mathrm{d}f)\\ &= \int_{\mathcal{C}} 1_{\{f\in A\}}1_{\{f(x_0)>0\}}\mu(\mathrm{d}f).\end{aligned}$$

Here, we use successively (5), the change of variable $\tilde\zeta = \zeta/f(x_0)$ with $f(x_0) > 0$ and (4) for the last equality. □

Proof of Theorem 1. The distribution of $\phi^+_{x_1}$ is given in Proposition 1. We prove the result for the conditional distribution of $\phi^+_{x_{n+1}}$ given $(\phi^+_{x_i})_{i=1,\dots,n}$. Recall that $\Phi^+_n = \{\phi^+_{x_1}, \dots, \phi^+_{x_n}\}$. Then, by Lemma 3.2 in Dombry & Éyi-Minko (2012), the conditional distribution of Φ^-_n given Φ^+_n is equal to the distribution of a Poisson process with intensity

$$1_{\{f(x_i)<Z(x_i),\ i=1,\dots,n\}}\mu(\mathrm{d}f) = 1_{\{f(x_i)<Z_n(x_i),\ i=1,\dots,n\}}\mu(\mathrm{d}f), \tag{A1}$$

where the equality follows from (8). In order to determine $\phi^+_{x_{n+1}}$ we focus on the functions $\phi \in \Phi^-_n$ satisfying $\phi(x_{n+1}) > Z_n(x_{n+1})$ and consider the restriction

$$\tilde\Phi_{n+1} = \Phi^-_n \cap \{f \in \mathcal{C}, f(x_{n+1}) > Z_n(x_{n+1})\}.$$

It follows from (A1) that conditionally on $(\phi^+_{x_i})_{1\le i\le n}$, $\tilde\Phi_{n+1}$ is a Poisson process with intensity given by (9). We distinguish two cases. If $\tilde\Phi_{n+1} = \emptyset$ then there is no function in Φ^-_n exceeding Z_n at point x_{n+1}, that is, $Z(x_{n+1}) = Z_n(x_{n+1})$ and $\phi^+_{x_{n+1}} = \mathrm{argmax}_{\phi\in\Phi^+_n}\phi(x_{n+1})$. If $\tilde\Phi_{n+1} \neq \emptyset$ then there is some function in Φ^-_n exceeding Z_n at point x_{n+1}, that is, $Z(x_{n+1}) > Z_n(x_{n+1})$ and $\phi^+_{x_{n+1}} = \mathrm{argmax}_{\phi\in\tilde\Phi_{n+1}}\phi(x_{n+1})$. This concludes the proof of Theorem 1. □

Proof of Theorem 2. For any $k = 1, \dots, N$, (5) implies

$$\textstyle\int_{\mathcal{C}} f(x_k)1_{\{f(x)/\|f(x)\|\in A\}}\,\nu(\mathrm{d}f) = \int_{\mathcal{C}} 1_{\{f(x)/\|f(x)\|\in A\}}\,P_{x_k}(\mathrm{d}f). \tag{A2}$$

We compute the μ_x-measure of the set $U^{-1}\{(u,\infty)\times A\}$ for $u > 0$ and a Borel set $A \subset S_{N-1}$,

$$\begin{aligned}\mu_x[U^{-1}\{(u,\infty)\times A\}] &= \int_{\mathcal{C}}\int_0^\infty 1_{\{\zeta\|f(x)\|>u\}}1_{\{f(x)/\|f(x)\|\in A\}}\zeta^{-2}\mathrm{d}\zeta\,\nu(\mathrm{d}f)\\ &= \frac{1}{u}\int_{\mathcal{C}}\|f(x)\|1_{\{f(x)/\|f(x)\|\in A\}}\,\nu(\mathrm{d}f) = \frac{1}{u}\sum_{k=1}^N\int_{\mathcal{C}} f(x_k)1_{\{f(x)/\|f(x)\|\in A\}}\,\nu(\mathrm{d}f)\end{aligned}$$

$$= \frac{1}{u}\sum_{k=1}^{N}\int_{\mathcal{C}} 1_{\{f(x)/\|f(x)\|\in A\}}\, P_{x_k}(\mathrm{d}f) = \frac{N}{u}\frac{1}{N}\sum_{k=1}^{N}\int_{\mathcal{C}} 1_{\{f(x)/\|f(x)\|\in A\}}\, P_{x_k}(\mathrm{d}f), \qquad \text{(A3)}$$

where the penultimate equality follows from (A2). Let $Y^{(k)}$ $(k = 1, \ldots, N)$, be independent random processes with distribution P_{x_k}, respectively, and let T be an independent uniform random variable on $\{1, \ldots, N\}$, then (A3) can be restated as

$$\mu_x[U^{-1}\{(u,\infty)\times A\}] = \frac{N}{u}\mathrm{pr}\left\{\frac{Y^{(T)}(x)}{\|Y^{(T)}(x)\|}\in A\right\}.$$

Comparing this with (10) yields the assertion of the theorem. □

REFERENCES

BLANCHET, J. & DAVISON, A. C. (2011). Spatial modeling of extreme snow depth. *Ann. Appl. Stat.* **5**, 1699–1725.

BOLDI, M.-O. (2009). A note on the representation of parametric models for multivariate extremes. *Extremes* **12**, 211–218.

BOLDI, M.-O. & DAVISON, A. C. (2007). A mixture model for multivariate extremes. *J. R. Stat. Soc. Ser. B Stat. Methodol.* **69**, 217–229.

BUISHAND, T. A., DE HAAN, L. & ZHOU, C. (2008). On spatial extremes: with application to a rainfall problem. *Ann. Appl. Stat.* **2**, 624–642.

CAPÉRAÀ, P., FOUGÈRES, A.-L. & GENEST, C. (2000). Bivariate distributions with given extreme value attractor. *J. Multivariate Anal.* **72**, 30–49.

COLES, S. G. (1993). Regional modelling of extreme storms via max-stable processes. *J. R. Stat. Soc. Ser. B Stat. Methodol.* **55**, 797–816.

DAVISON, A. C., PADOAN, S. A. & RIBATET, M. (2012). Statistical modeling of spatial extremes (with discussion). *Statist. Sci.* **27**, 161–186.

DE HAAN, L. (1984). A spectral representation for max-stable processes. *Ann. Probab.* **12**, 1194–1204.

DIEKER, A. B. & MIKOSCH, T. (2015). Exact simulation of Brown–Resnick random fields at a finite number of locations. *Extremes* **18**, 301–314.

DOMBRY, C. & ÉYI-MINKO, F. (2012). Strong mixing properties of max-infinitely divisible random fields. *Stochastic Process. Appl.* **122**, 3790–3811.

DOMBRY, C. & ÉYI-MINKO, F. (2013). Regular conditional distributions of continuous max-infinitely divisible random fields. *Electron. J. Probab.* **18**, 1–21.

DOMBRY, C., ÉYI-MINKO, F. & RIBATET, M. (2013). Conditional simulation of max-stable processes. *Biometrika* **100**, 111–124.

ENGELKE, S., KABLUCHKO, Z. & SCHLATHER, M. (2011). An equivalent representation of the Brown–Resnick process. *Statist. Probab. Lett.* **81**, 1150–1154.

ENGELKE, S., MALINOWSKI, A., KABLUCHKO, Z. & SCHLATHER, M. (2015). Estimation of Hüsler–Reiss distributions and Brown–Resnick processes. *J. R. Stat. Soc. Ser. B Stat. Methodol.* **77**, 239–265.

ENGELKE, S., MALINOWSKI, A., OESTING, M. & SCHLATHER, M. (2014). Statistical inference for max-stable processes byconditioning on extreme events. *Adv. Appl. Probab.* **46**, 478–495.

GHOUDI, K., KHOUDRAJI, A. & RIVEST, L.-P. (1998). Propriétés statistiques des copules de valeurs extrêmes bidimensionnelles. *Canad. J. Statist.* **26**, 187–197.

GUDENDORF, G. & SEGERS, J. (2010). Extreme-value copulas. In *Copula Theory and its Applications*, P. Jaworski, F. Durante, W. K. Härdle & T. Rychlik, eds., vol. 198 of *Lecture Notes in Statistics – Proceedings*. Springer, Heidelberg, pp. 127–145.

HÜSLER, J. & REISS, R.-D. (1989). Maxima of normal random vectors: between independence and complete dependence. *Statist. Probab. Lett.* **7**, 283–286.

KABLUCHKO, Z. (2011). Extremes of independent Gaussian processes. *Extremes* **14**, 285–310.

KABLUCHKO, Z., SCHLATHER, M. & DE HAAN, L. (2009). Stationary max-stable fields associated to negative definite functions. *Ann. Probab.* **37**, 2042–2065.

OESTING, M., KABLUCHKO, Z. & SCHLATHER, M. (2012). Simulation of Brown–Resnick processes. *Extremes* **15**, 89–107.

OESTING, M. & SCHLATHER, M. (2014). Conditional sampling for max-stable processes with a mixed moving maxima representation. *Extremes* **17**, 157–192.

OPITZ, T. (2013). Extremal t processes: Elliptical domain of attraction and a spectral representation. *J. Multivar. Anal.* **122**, 409–413.

RESNICK, S. I. (2008). *Extreme Values, Regular Variation and Point Processes*. New York: Springer.

SCHLATHER, M. (2002). Models for stationary max-stable random fields. *Extremes* **5**, 33–44.